

## Electronic Supporting Information

of

### Characterizations of the thermal/thermal oxidative stability of fluorinated graphene with various structures

Wenchuan Lai, Dazhou Xu, Xu Wang, Zaoming Wang, Yang Liu, Xiaojiao Zhang and Xiangyang

Liu\*

State Key Laboratory of Polymer Materials Engineering, College of Polymer Science and Engineering, Sichuan University, Chengdu, Sichuan, 610065, P.R. China;

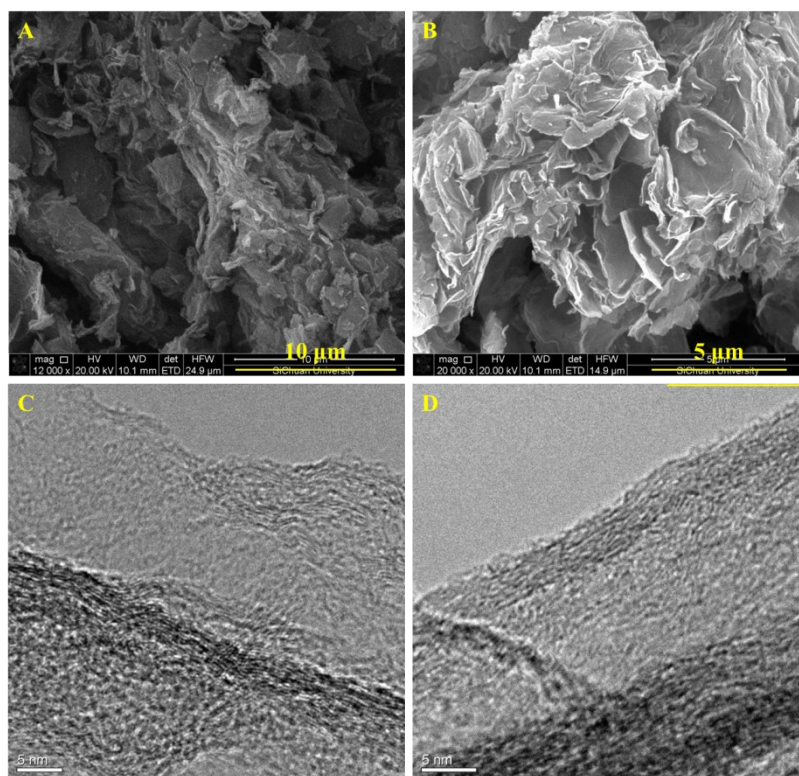


**Fig. S1** SEM and TEM images of graphene (G) and fluorinated graphene (FG). (A) SEM image of G, (B) SEM image of FG, (C) TEM image of G, (D) TEM image of FG.

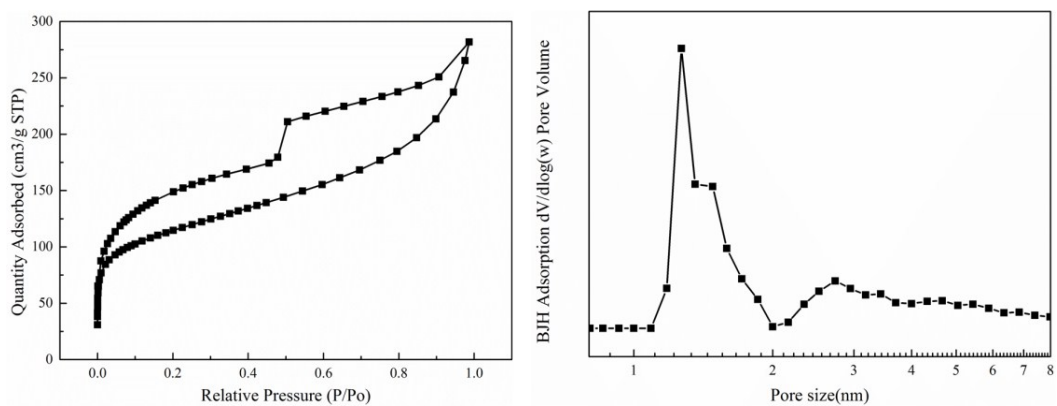


**Fig. S2** Nitrogen sorption isotherms and pore-size distributions (PSDs) of graphene

The surface area of raw graphene is 403.9 m<sup>2</sup>/g calculated from BET data.

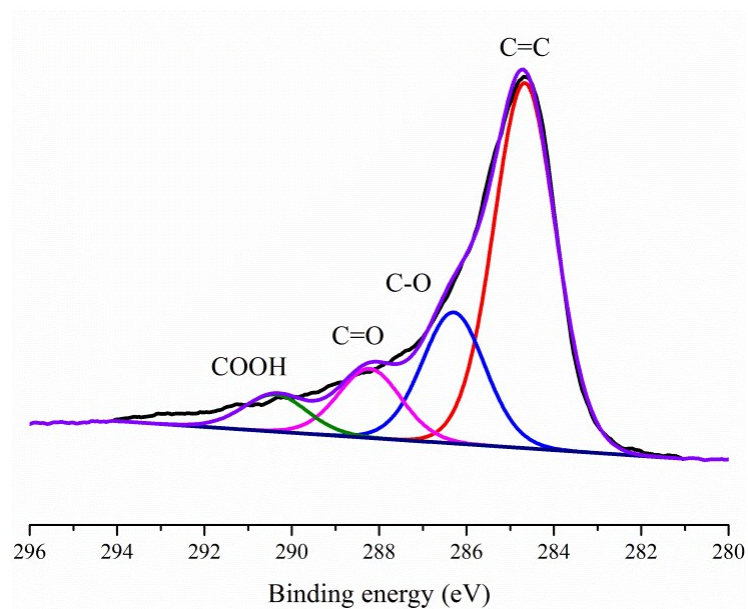


**Fig. S3** Curve fitting of XPS C 1s spectrum of raw graphene.

**Table S1** The chemical composition of FG and FPG based on XPS calculations.

Fluorinated graphene	G	FG1	FG2	FG3	FG4	FG5	FG6	PG	FPG1	FPG2	FPG3
F/C ratio	0	0.07	0.23	0.41	0.69	0.95	1.12	0	0.30	0.48	0.55
Semi-ionic C-F/all C atoms (%)	0	11.4 4	20.68	12.1	4.05	0	0	0	0	0	0.78
Covalent C-F/all C atoms (%)	0	5.71	14.21	32.34	45.16	48.91	55.5	0	30.39	43.23	46.50
CF <sub>2</sub> /all C atoms (%)	0	2.17	5.95	11.15	13.61	13.45	14.25	0	1.69	1.93	2.12
CF <sub>3</sub> /all C atoms (%)	0	1.26	2.15	3.48	7.59	6.91	2.59	0	2.51	2.39	1.57

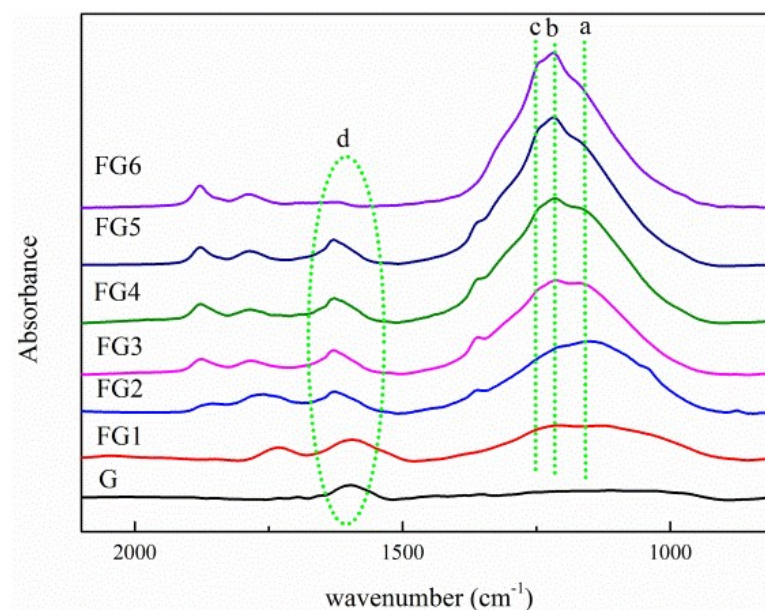


**Fig. S4** FT-IR spectra of FG recorded between 800 and 2100  $\text{cm}^{-1}$ , The peak **a** is at around 1120  $\text{cm}^{-1}$ , peak **b** at 1210  $\text{cm}^{-1}$ , peak **c** at 1256  $\text{cm}^{-1}$  and peak **d** at 1637  $\text{cm}^{-1}$ .

In the FT-IR spectra of FG (**Fig. S4**), the intensity of peak **d** assigned to the aromatic carbons in the region of 1510 ~ 1700  $\text{cm}^{-1}$  firstly changes little as fluorine content increases, and only up to

the very high F/C ratio (1.12) does it weaken. The broad absorption region from 1100 ~ 1300  $\text{cm}^{-1}$  is attributed to the stretching vibrations of C-F bonds of FG samples, which was obviously enhanced as the fluorination deepening. In detail, the ratio of peak b to peak a, or the ratio of covalent C-F bond at 1211  $\text{cm}^{-1}$  to semi-ionic C-F bond at 1161  $\text{cm}^{-1}$ , was firstly decreased and then increased as F/C ratio rising, consistent with the result in XPS C 1s spectra, as well as for the enhancement of peak c at 1247  $\text{cm}^{-1}$  assigned to  $\text{CF}_2$  groups.

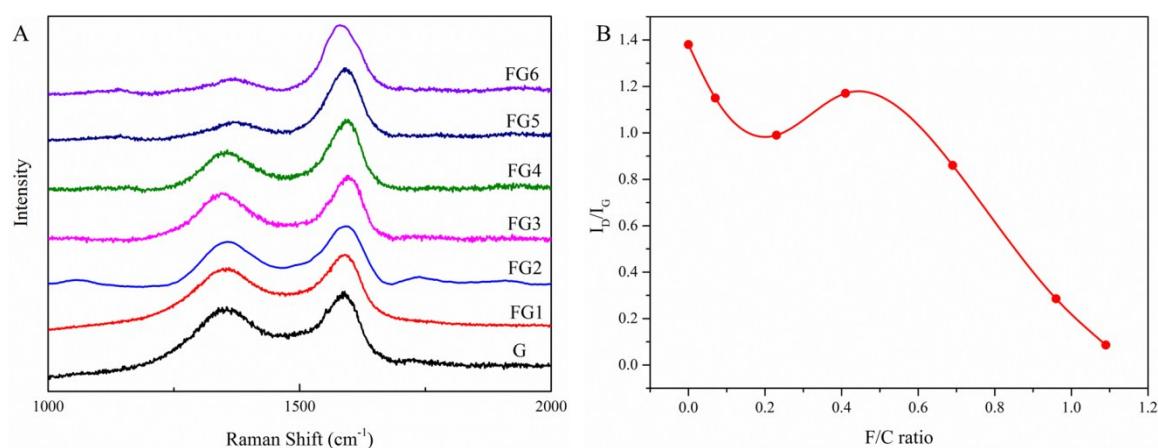


**Fig. S5** Raman spectra of FG samples with various F/C ratio.

There are two typical Raman spectrum features of graphene or graphene derivatives: the D band and the G band. The D band is due to the breathing modes of k-point phonons of  $A_{1g}$  symmetry which is originated from the phonon scattering effect at the interface between the localized graphite domain and disordered regions, while the G band is usually assigned to the  $E_{2g}$  phonon of  $\text{sp}^2$  carbons.<sup>1</sup> The detailed evolutions of Raman spectra for fluorinated graphene with different F/C ratio were complicated as **Fig. S5** depicted. The  $I_D/I_G$  ratio didn't exhibit a change

with the monotonic tendency that it decreased some for first fluorination stage, increased a little for second fluorination stage and continued declining for the third stage. It seemed to be confused for the change of  $I_D/I_G$  at first stage but if we ignored that, the evolutions at next two stages were more unambiguous and almost consistent with the research reported previously. The foregoing fluorination would bring about the decrease of  $sp^2$  carbons and the partial expansion of disordered  $C_{sp2}$  domains, which thus made the  $I_D/I_G$  ratio rise. While the further fluorination broke the conjugated system into small aromatic piece, and some of piece with a size below 25 nm which is the structure foundation of D band, and therefore the  $I_D/I_G$  ratio started to decline gradually.

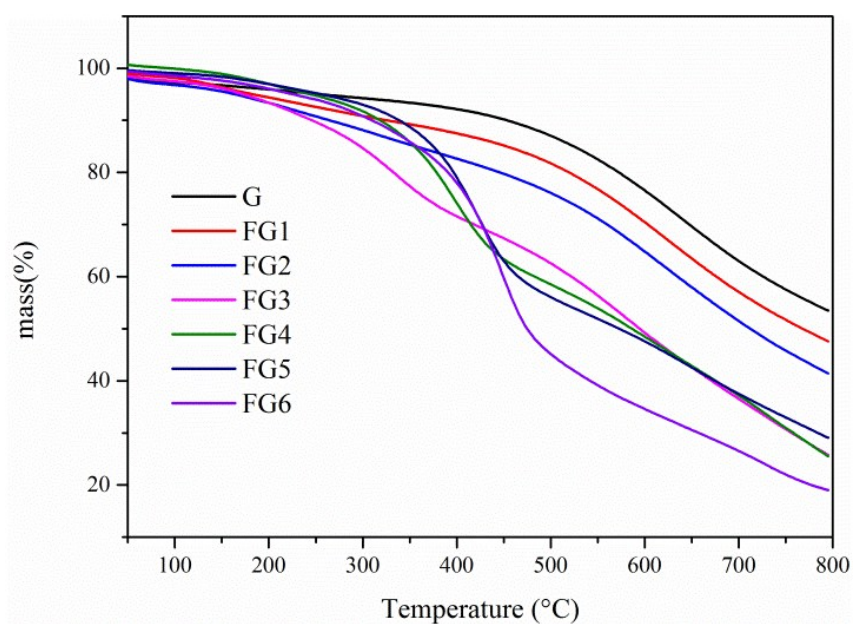


**Fig. S6** TGA curves of FG samples at heating rate of 10 °C/min under  $N_2$  atmosphere.

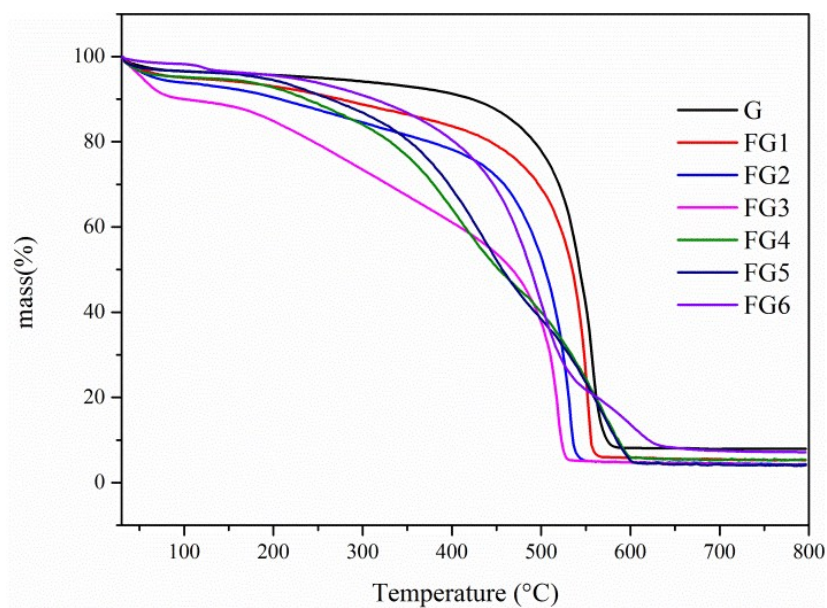


**Fig. S7** TGA curves of FG samples at heating rate of 10 °C/min under air atmosphere.

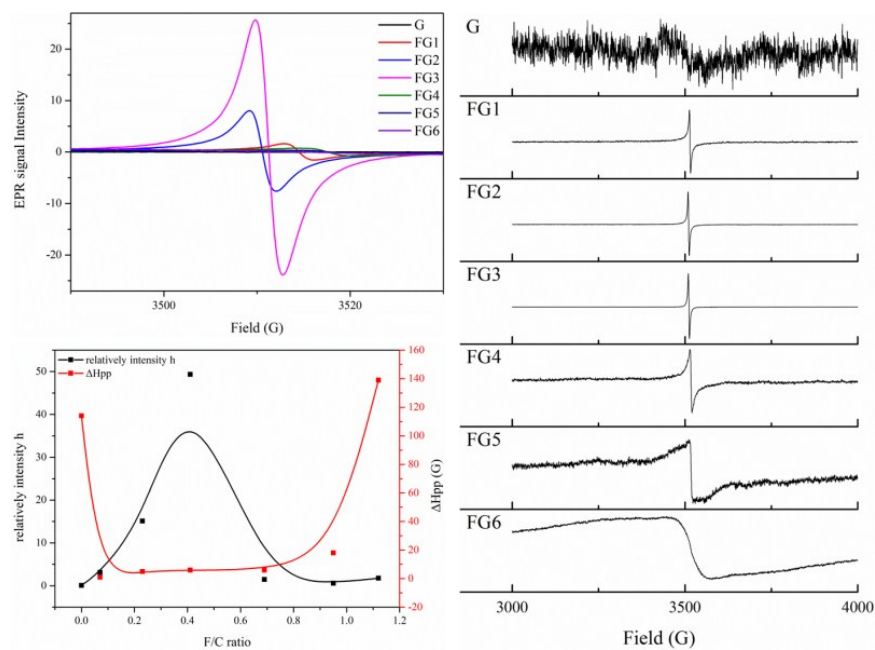


**Fig. S8.** EPR spectra of FG with different F/C ratio.

**Fig. S8** shows changes in EPR spectra of FG with different F/C ratio, and samples were stored under N<sub>2</sub> atmosphere for some time. All samples except for raw graphene show evident

EPR signals in the region of  $g$ -factor $\sim 2$ , which is the typical for free radicals and paramagnetic structural defects of carbon material. As the F/C ratio increases, the relatively intensity of EPR signal, which is proportional to the total amount of corresponding spin centers, firstly increases drastically and then decreases drastically as well. The  $\Delta H_{pp}$  value of EPR signal firstly remains small, ranging from 1-18 G for FG1-FG5, while increases quickly to 139 G for FG6. No hyperfine splitting lines like the EPR signal of fluorinated graphite were observed.<sup>2</sup>

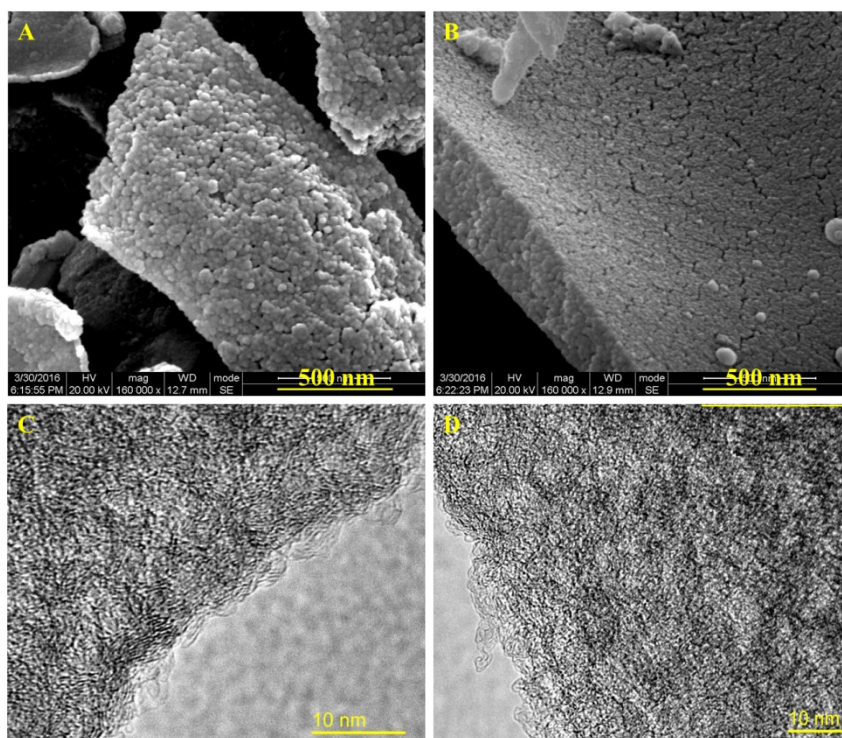


**Fig. S9** SEM and TEM images of graphene (PG) and fluorinated graphene (FPG). (A) SEM image of PG, (B) SEM image of FPG, (C) TEM image of PG, (D) TEM image of FPG.

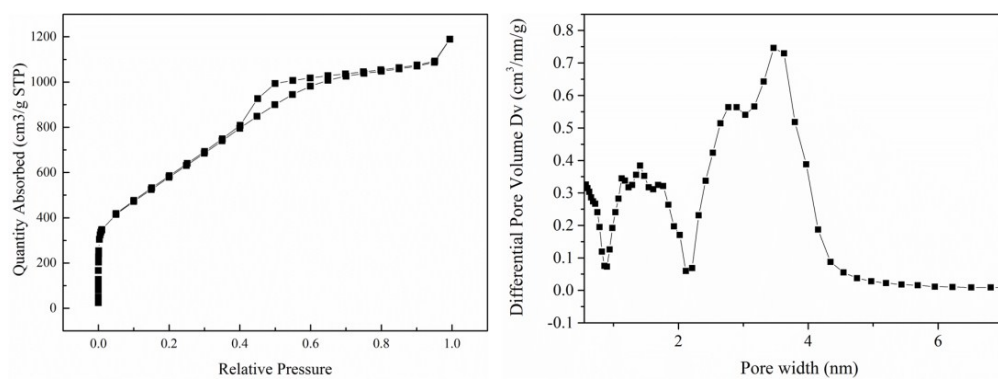


**Fig. S10** Nitrogen sorption isotherms and pore-size distributions (PSDs) of porous graphene

The surface area of raw graphene is 2193.305 m<sup>2</sup>/g calculated from BET data.

**Table S2** The binding energy in XPS spectra of FPG samples

Samples	Binding Energy of covalent	Binding Energy of main
	C-F bonds in XPS C 1s spectra (eV)	peak in XPS F 1s spectra (eV)
PG	/	/
FPG1	289.18	687.68
FPG2	289.58	688.08
FPG3	289.78	688.28

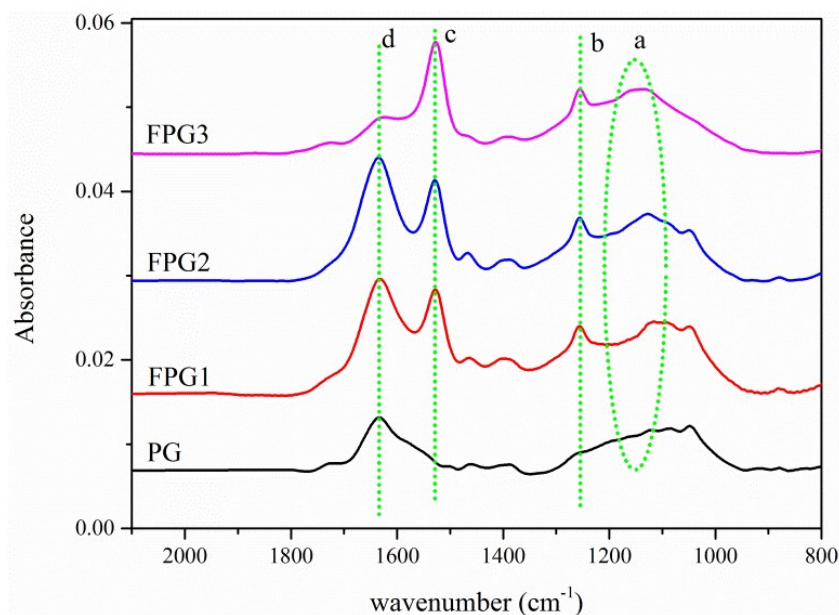


**Fig. S11** FT-IR spectra of fluorinated porous graphene recorded between 800 and 2100  $\text{cm}^{-1}$ , The peak a is at around 1130  $\text{cm}^{-1}$ , peak b at 1256  $\text{cm}^{-1}$ , peak c at 1522  $\text{cm}^{-1}$  and peak d at 1637  $\text{cm}^{-1}$ .

**Fig. S11** depicts the FT-IR spectra of various fluorinated porous graphene. The broad absorption region from 1100-1300  $\text{cm}^{-1}$  was assigned to the stretching vibrations of C-F bonds, while the peak c and peak d in the region of 1500-1700  $\text{cm}^{-1}$  were attributed the C=C bonds vibrations of FPG. Besides, peak c at 1254  $\text{cm}^{-1}$  was usually observed in FTIR spectra for graphitized carbon fluorides prepared at low temperature, however whose assignment has been uncertain until now.

The intensity of peak a belonged to C-F bonds was obviously enhanced after the fluorination of porous graphene, and the position of which was gradually shifted to the higher wavenumber region, from 1120 $\text{cm}^{-1}$  to 1127 $\text{cm}^{-1}$  and 1140 $\text{cm}^{-1}$  as F/C ration rising. However, the absorption peak of C=C bonds (c and d) shows something strange that the peak at 1630 $\text{cm}^{-1}$  weakens while peak at 1530 $\text{cm}^{-1}$  strengthens, probably explained by that two peaks may attributed to the different

C=C existing in aromatic region ( $1530\text{cm}^{-1}$ ) or the isolated olefin ( $1630\text{cm}^{-1}$ ), respectively.

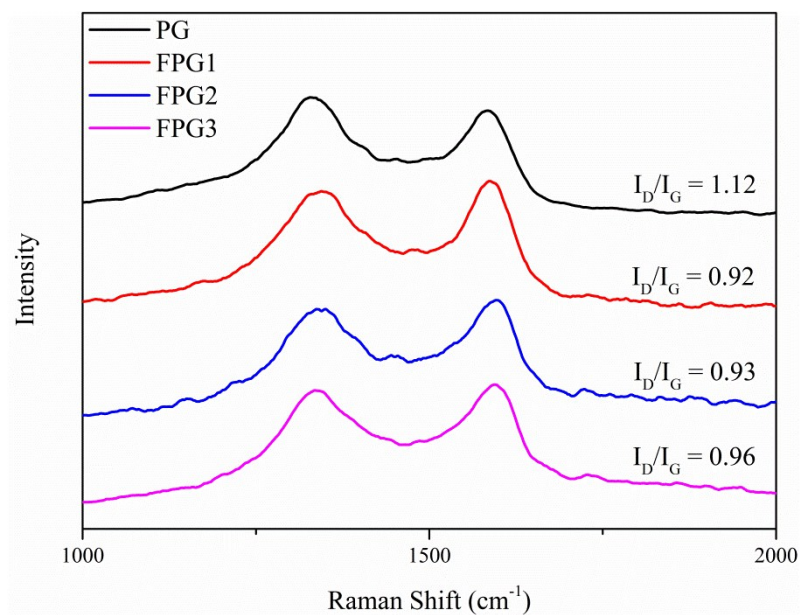


**Fig. S12** Raman spectra of FPG samples with various F/C ratios.

The change tendency of I<sub>D</sub>/I<sub>G</sub> ratio of PG and FPG samples was similar to G ~ FG3 samples. Since the further defluorination of porous graphene (PG) seemed to be difficult under the same condition as graphene (G), the I<sub>D</sub>/I<sub>G</sub> ratio of FPG samples has not shown an further decreasing tendency unless F/C ratio higher than 0.5.

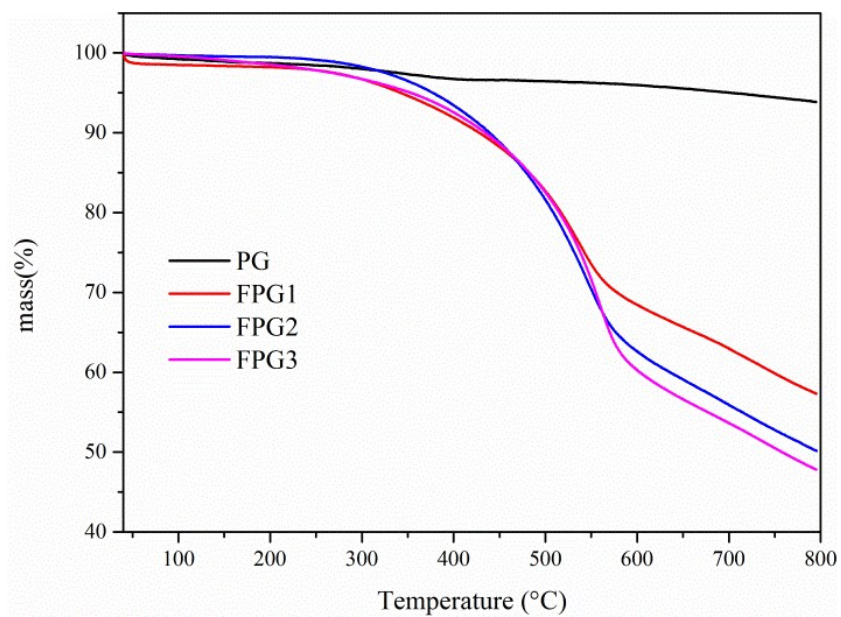


**Fig. S13** TGA curves of FPG samples at heating rate of 10 °C/min under N<sub>2</sub> atmosphere.

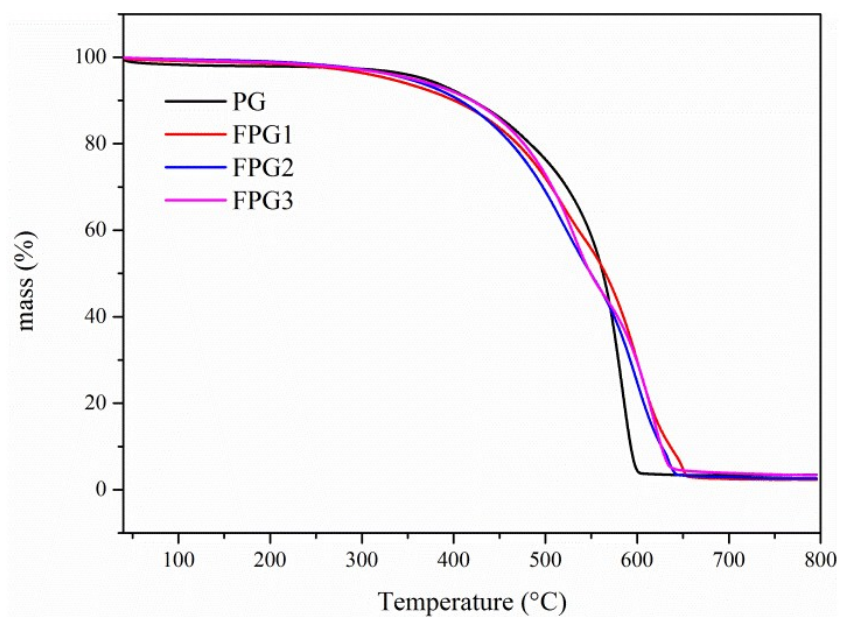


**Fig. S14** TGA curves of FPG samples at heating rate of 10 °C/min under air atmosphere.

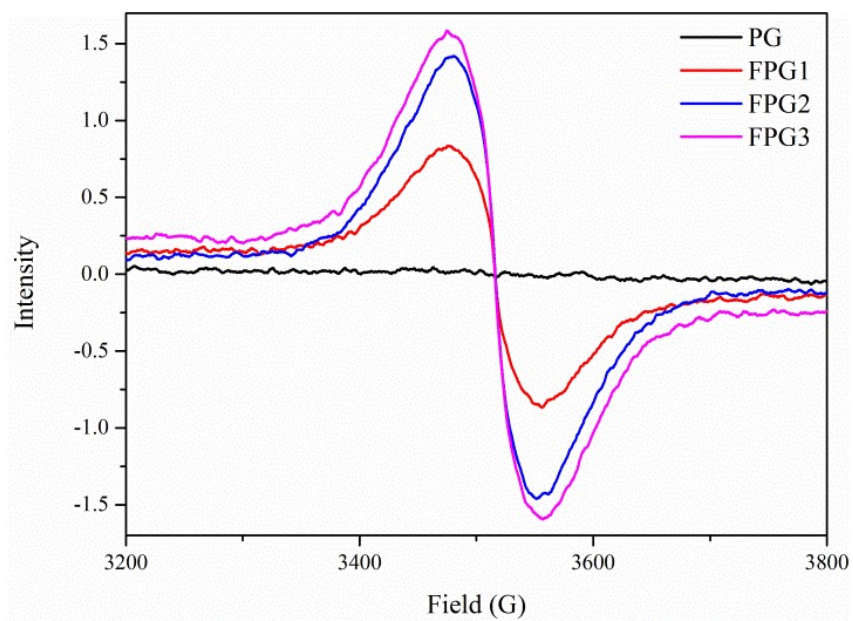


**Fig. S15** EPR spectra of fluorinated porous graphene with different fluorine content.

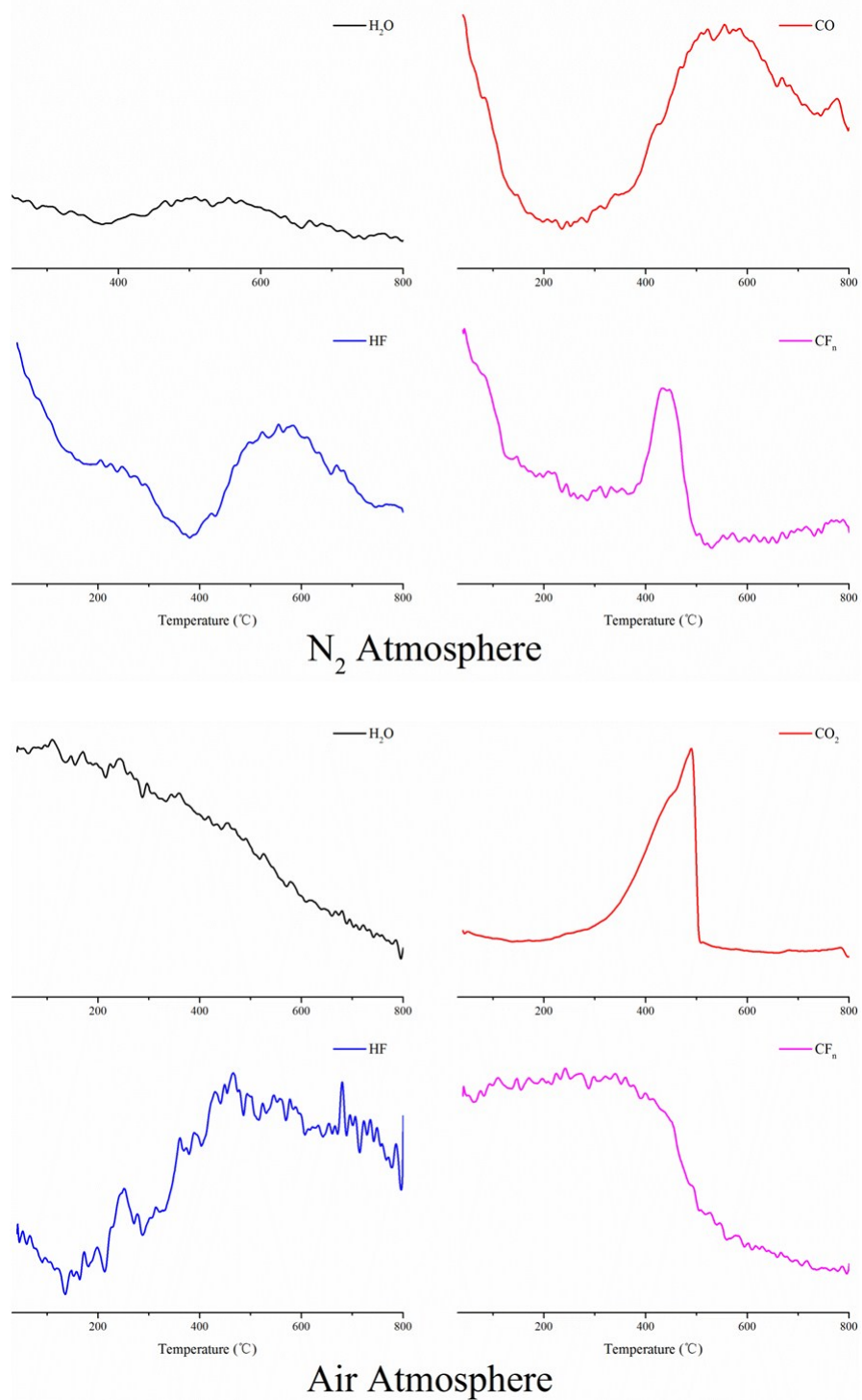


**Fig. S16** TGA-IR Hyphenation spectra of FG6 under N<sub>2</sub> and air atmosphere.

TGA-IR Hyphenation was performed to investigate the generated fragments during thermal decomposition with a temperature RT-800 °C at heat rate of 10 °C/min under N<sub>2</sub> and air

atmosphere. The pyrolysis species whose intensities would be depended on temperature, were identified by the absorption wavenumber in infrared spectrum, with 2349, 1659, 2150, 3839 and 1152  $\text{cm}^{-1}$  for  $\text{CO}_2$ ,  $\text{H}_2\text{O}$ ,  $\text{CO}$ ,  $\text{HF}$  and  $\text{CF}_n$  species respectively.

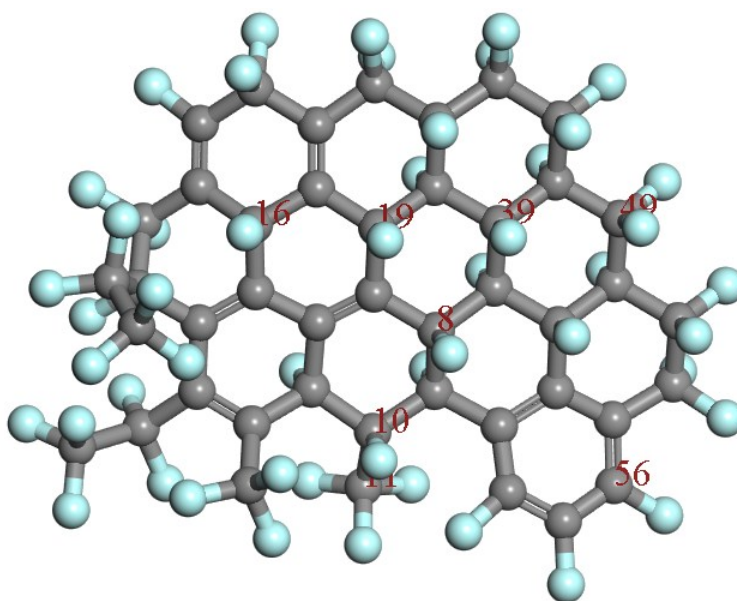


**Fig. S17** The model molecule for DFT calculations using Dmol3.

**Table S3** The bond length of diverse C-F bonds in model molecular based on DFT calculations, the serial number of carbon is corresponding to **Fig. S17**.

<b>C-F bond</b>	<b>Number of unsaturated carbons in <math>\alpha</math> position</b>	<b>Bond length (Angstrom)</b>
<b>C<sub>16</sub>-F</b>	3	1.465
<b>C<sub>19</sub>-F</b>	2	1.425
<b>C<sub>8</sub>-F</b>	1	1.412

<b>C<sub>39</sub>-F</b>	0	1.391
<b>C<sub>10</sub>-F (edge)</b>	0	1.383
<b>C<sub>49</sub>-F<sub>2</sub> (edge)</b>	0	1.369
<b>C<sub>11</sub>-F<sub>3</sub> (edge)</b>	0	1.364
<b>C<sub>56</sub>-F (edge)</b>	aromatic C-F bond	1.344

After heating bath by dynamics simulation

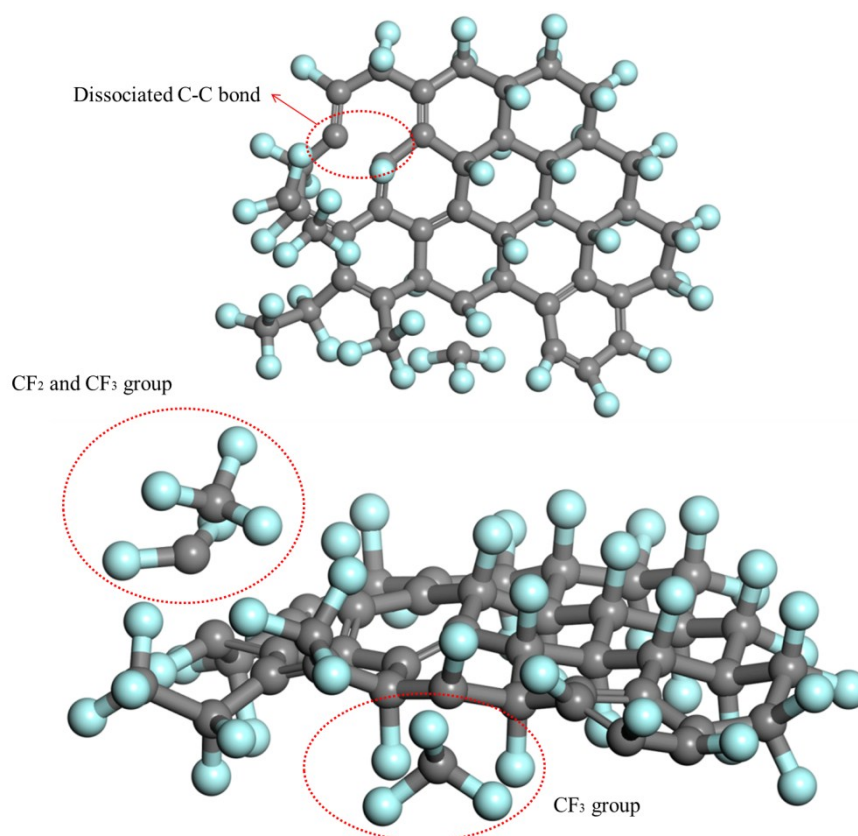


**Fig. S18** Structure changes of model molecule after heating bath at 800 K by dynamics simulation

## References

1. A. C. Ferrari, *Solid state communications*, 2007, **143**, 47-57.
2. M. Panich, A. I. Shames and T. Nakajima, *Journal of Physics and Chemistry of Solids*, 2001, **62**, 959-964.